Published in final edited form as:

*J Biol Inorg Chem*. 2016 October ; 21(7): 825–836. doi:10.1007/s00775-016-1381-8.

# Iron–sulfur cluster exchange reactions mediated by the human Nfu protein

**Christine Wachnowsky**[#1,2], **Insiya Fidai**[#1,3], and **J. A. Cowan**[1,2,3]

[1] Department of Chemistry and Biochemistry, The Ohio State University, 100 West 18th Avenue, Columbus, OH 43210, USA

[2] The Ohio State Biochemistry Program, The Ohio State University, Columbus, USA

[3] The Biophysics Graduate Program, The Ohio State University, Columbus, USA

[#] These authors contributed equally to this work.

## Abstract

Human Nfu is an iron–sulfur cluster protein that has recently been implicated in multiple mitochondrial dysfunctional syndrome (MMDS1). The Nfu family of proteins shares a highly homologous domain that contains a conserved active site consisting of a CXXC motif. There is less functional conservation between bacterial and human Nfu proteins, particularly concerning their Iron–sulfur cluster binding and transfer roles. Herein, we characterize the cluster exchange chemistry of human Nfu and its capacity to bind and transfer a [2Fe–2S] cluster. The mechanism of cluster uptake from a physiologically relevant [2Fe–2S] $(GS)_4$ cluster complex, and extraction of the Nfu-bound iron–sulfur cluster by glutathione are described. Human holo Nfu shows a dimer-tetramer equilibrium with a protein to cluster ratio of 2:1, reflecting the Nfu-bridging [2Fe–2S] cluster. This cluster can be transferred to apo human ferredoxins at relatively fast rates, demonstrating a direct role for human Nfu in the process of [2Fe–2S] cluster trafficking and delivery.

### Keywords

Mitochondrial disease; Metalloprotein; Iron–sulfur cluster; Cluster exchange; Nfu

## Introduction

Iron–sulfur clusters are essential cofactors that are found in all kingdoms of life and have demonstrated unique functional roles throughout evolution [1]. In vivo they are required for important roles that include electron transport, structural stabilization, sensing of environmental factors, transcriptional and translational regulation, and substrate binding in catalysis [2]. The assembly of iron–sulfur clusters is complex because iron and sulfur would be toxic if allowed to freely exist in the cell [3, 4], and so an array of ancillary proteins is

J. A. Cowan cowan@chemistry.ohio-state.edu.

**Electronic supplementary material** The online version of this article (doi:10.1007/s00775-016-1381-8) contains supplementary material, which is available to authorized users.

required to synthesize and mobilize such cofactors. How these function at the molecular level is not fully understood. Multiple pathways have been identified for iron–sulfur cluster biosynthesis, depending on the organism, and consist of three main classes of gene cluster: namely the Isc (iron–sulfur cluster), Nif (nitrogen fixation) and Suf (sulfur utilization factor) systems [3]. Of these three, the Isc-related protein network is the major housekeeping pathway for Fe–S cluster biosynthesis [5] by assembly on a scaffold protein with subsequent transfer to target proteins, either by the means of intermediate assembly/transport proteins, or chaperone proteins that mediate delivery [4].

One such iron–sulfur cluster assembly protein, Nfu, also known as HIRIP5 (HIRA interacting protein, where HIRA is the histone cell cycle regulation homologue A) [6], has generated much interest recently as a result of its involvement in multiple mitochondrial dysfunction syndrome (MMDS) [7]. A single point mutation in human Nfu near the active site causes MMDS1, which results in patient death before age two from downstream functional impairments of target iron–sulfur cluster proteins [8–10]. Despite the role of Nfu in MMDS1 and its potential role in histone regulation, little is known about the functional chemistry and cluster binding properties of human Nfu.

The Nfu protein family demonstrates high sequence conservation between prokaryotes and eukaryotes in the domain carrying a pair of cluster-binding cysteines in the C- or N-terminal domain, depending on the protein [11]; however the actual function of the protein appears to be less conserved as major differences have been identified in both the nuclearity and role of the iron–sulfur center, comparing *Synechocystis* PCC6803, *Escherichia coli* and *Arabidopsis thaliana* proteins [11–14]. These differences make it difficult to predict the cellular function of human Nfu. Recent reports have shed light on the tertiary structure [15, 16] and cellular localization of human Nfu, but it's in vivo function is not well understood [17, 18].

Nfu proteins typically consist of multiple domains, of which one is always an “Nfu” domain containing a conserved CXXC motif that is crucial for function in iron–sulfur cluster biosynthesis and trafficking [11]. The domain organization differs among organisms, indicating that the role of Nfu has changed during the process of evolution, but the functional CXXC motif has remained conserved. In humans, the Nfu protein consists of two domains: an N-terminal and a C-terminal domain, where the C-terminal domain is the Nfu domain. However, this C-terminal domain also exhibits conformational flexibility [15, 16], and so the structure–function relationship of the C-terminal domain of Nfu is complex in terms of its intracellular role.

Human Nfu exists in two isoforms, one of which is mitochondrial and the other is cytosolic [17]. The main difference between the two isoforms is the presence or absence of the mitochondrial targeting domain. Therefore, both domains exhibit the same structural features. However, the specific function of human Nfu and how it may contribute to iron–sulfur cluster biosynthesis is unknown. Following a low yielding reconstitution with iron and inorganic sulfide, a [4Fe–4S] cluster form has been reported [17], as well as a role in the delivery of free sulfide for iron–sulfur cluster biosynthesis [19]. Most likely, human Nfu is involved in multiple cellular pathways that underlie its role in MMDS1. It is essential to fully understand the Fe–S cluster chemistry associated with human Nfu to better understand

the cellular impact that can result from this form of disease. Holo Nfu is believed to take the form of a cluster-bridged dimer, and prior reports of cluster transfer activity for Nfu proteins implicate both [2Fe–2S] and [4Fe–4S] cluster forms [13]. Herein we report the results of investigations directed toward understanding structure–function relationships of human Nfu, characterizing its iron–sulfur cluster binding capabilities, and illustrating a novel mechanism of reconstitution via a glutathione-complexed iron–sulfur cluster ($[2Fe–2S](GS)_4$ [20]. We have previously proposed the latter to be a component of the labile iron pool and a possible substrate for the mitochondrial ABCB7 exporter.

## Materials and methods

### Materials

PD10 desalting columns were purchased from GE Health-care. Ferric chloride, sodium sulfide, DTT (Dithiothreitol), TCEP (Tris (2-carboxy-ethyl) phosphine) and l-cysteine were purchased from Fisher.

### Protein expression and purification

Purification of *Thermotoga maritima (Tm)* Nifs was performed as previously reported [21, 22]. The expression vector for human ferredoxin-1 (*Homo sapiens (Hs)* Fdx1) was kindly provided by Dr. J. Markley and protein was expressed and purified according to literature procedures [23]. Briefly, *Hs* Fdx1 was purified using DE-52 anion exchange column followed by FPLC purification with a size exclusion Superose-12 column (HR 16/50, Pharmacia) run at 0.2 mL/min with 50 mM HEPES, 100 mM NaCl, pH 7.5 at 4 °C. All the colored fractions were collected and combined. Purification for human ferredoxin-2 (*Hs* Fdx2) was performed as previously reported [24], using a TALON column, as it is his-tagged. Protein was eluted with a buffer containing 50 mM HEPES, 100 mM NaCl, 150 mM imidazole, pH 7.5 and concentrated by amicon ultrafiltration over a 10 kDa membrane. Protein purity for both the ferredoxins was assayed by use of a 12 % SDS-PAGE gel that was visualized with Coomassie Blue staining. The ferredoxins purified as holo proteins and were then subsequently converted to apo forms by treatment with 100 mM EDTA, 5 mM DTT and 8 M urea in a buffered solution, pH 7.5.

Full length human Nfu in a pET28(b +) vector in *E. coli* strain BL21(DE3) host cells was grown overnight in 10 ml of Luria–Bertani (LB) broth media with kanamycin (50 μM) at 37 °C [19]. The overnight cultures were diluted 1:1000 in LB media containing 50 μM kanamycin until the $OD_{600}$ reached 0.6. At this point, protein expression was induced with 0.5 mM of isopropyl β-D-1-thiogalactopyranoside (IPTG), and cultures were incubated overnight at 37 °C. Cell pellets were collected by centrifugation at 4330*g* for 15 min at 4 °C, and resuspended in 30 ml of 50 mM HEPES, 100 mM NaCl, pH 7.5. Resuspended pellets were incubated with 30 mg lysozyme and 0.6 mg DNase I for 30 min at 4 °C and lysed by use of a dismembranator. Cell lysate was centrifuged at 28,982*g* for 50 min at 4 °C, and the supernatant was applied to a TALON column. Protein was eluted with a buffer containing 50 mM HEPES, 100 mM NaCl, 150 mM imidazole, pH 7.5 and concentrated by amicon ultrafiltration over a 10 kDa membrane. Protein purity was assayed by use of a 12 % SDS-PAGE gel that was visualized with Coomassie Blue staining. Imidazole was removed by

dialysis at 4 °C against a buffer containing 50 mM HEPES, 100 mM NaCl, pH 7.5, and protein concentration was determined by the Bradford assay.

### Reconstitution of human Nfu

NifS-mediated in vitro reconstitution of Nfu [25] was completed as previously described. Briefly, argon purged ferric chloride and L-cysteine were added to an anaerobic mixture of approximately 200 μM purified Nfu, 2 μM *Tm* NifS, and 5 mM DTT to final concentrations of 1.6 mM $FeCl_3$ and 3.2 mM L-cysteine. The final solution was incubated for 1 h with stirring at room temperature, before separation of excess iron and sulfide through a PD-10 column that was equilibrated with an argon-purged solution of 50 mM HEPES, 100 mM NaCl, pH 7.5 in a Type B vinyl anaerobic chamber (Coy Laboratory Products Inc.), which uses a palladium catalyst and hydrogen gas mix of 5 %, providing a strict anaerobic atmosphere of >5 ppm $O_2$. Reconstituted protein was eluted with 3.5 ml of the equilibration buffer. The protein concentration was determined via the Bradford assay and the reconstitution of protein was confirmed by absorbance at 330 nm and 420 nm on a Cary WinUV Spectrophotometer.

### Structural analysis by circular dichroism (CD)

CD scans of apo and holo proteins were recorded on a JASCO J-815 CD spectrometer in a quartz 1 cm anaerobic cuvette. CD scans from 300 nm to 600 nm were collected to analyze signature cluster-bound protein peaks at a scan rate of 200 nm/min at 25 °C. Data were processed using JASCO Spectramanager II Analysis software and were represented in Origin 7.0.

### Oligomerization state determination by analytical ultracentrifugation (AUC)

Apo Nfu at 50 μM protein ($OD_{280}$ = 1.0), in the presence or absence of 1 mM TCEP, was loaded into the ultracentrifugation chambers and sealed, using 50 mM HEPES, 100 mM NaCl, pH 7.5 as a reference, with the addition of 1 mM TCEP and a 30 min incubation where needed. Reconstituted holo Nfu at 72 μM ($OD_{420}$ = 1.2) was loaded in the same manner with the same reference buffer. Samples were centrifuged at 45,000 rpm for 6 h to reach complete sedimentation. The sedimentation profiles were fit using SEDFIT to the Lamm equation [26, 27].

### $[Fe_2S_2](GS)_4$ synthesis

The cluster used was synthesized as previously reported [20]. Briefly, ferric chloride (20 mM) and sodium sulfide (20 mM) were added to 10 ml 40 mM glutathione solution, pH 8.6. A volume (40 ml) of ethanol was added to the mixture and mixed by vortexing. The precipitate was collected by centrifugation at 13,000 rpm for 10 min, washed twice with ethanol and dried under vacuum.

### Iron quantification [28, 29]

A solution of $[Fe_2S_2](GS)_4$ (0.05 mM, 200 μL) in $H_2O$ or holo protein was acidified by concentrated HCl (60 μL) and heated to 100 °C for 15 min. The resulting suspension was centrifuged at 14,000 rpm for 2 min and the supernatant (100 μL) was diluted with Tris–HCl

(0.5 M, 1.3 mL, pH 8.5). Solutions of sodium ascorbate (0.1 mL, 5 %) and bathophenanthroline-disulfonate (0.4 mL, 0.1 %) were sequentially added to the neutralized reaction solution with mixing between each addition. The solution was incubated at 25 °C for 1 h and iron was quantified by measuring the absorbance at 535 nm on a UV–vis spectrophotometer and calculated from a calibration curve made with 0.01–0.2 mM $FeCl_3$ standard solutions (Figure S1).

### Iron–sulfur cluster uptake monitored by CD

The ability of Nfu to take up an iron–sulfur cluster from the [2Fe–2S](GS)$_4$ complex was examined by circular dichroism (CD). CD scans were recorded on a JASCO J-815 CD spectrometer in a 1 cm anaerobic quartz cuvette from 600 to 300 nm at a scan rate of 200 nm/min at 25 °C, with a 2 min interval between each accumulation. Nfu (50 μM) in 50 mM HEPES, 100 mM NaCl pH 7.5, was thoroughly degassed in the presence of 5 mM DTT and transferred to the anaerobic cuvette. Solid [2Fe–2S](GS)$_4$ was resuspended in degassed 50 mM HEPES, 100 mM NaCl pH 7.5 and added to the argon-purged anaerobic cuvette via a gas-tight syringe to a final concentration of 100 μM to initiate the reaction. Spectra were processed using JASCO Spectramanager II Analysis software and were represented in Origin 7.0. The deconvolution function from Spectramanager II analysis software was used for analysis of bands in the spectra that contained overlapping Lorentzian curves having the same full width at half maximum value that accurately distinguishes the peak positions for each band.

Following observation of direct cluster uptake by Nfu, the concentration dependence of iron–sulfur cluster uptake by Nfu was determined by varying cluster concentration from 200 to 400 μM. Reconstitution of apo 50 μM Nfu was monitored from 358 to 368 nm at 10 s intervals over a period of 30 min. Initial rates were obtained for each of the cluster complex concentrations and were used to determine the overall second-order rate constant. Likewise, protein concentration dependence was determined by varying the concentration of apo Nfu from 25 to 150 μM, while monitoring cluster uptake from 300 μM cluster complex. The concentration dependence of excess glutathione was also examined using the same CD parameters by adding GSH to the apo reaction mixture and varying the concentration from 1 to 10 mM.

### Rate laws for cluster uptake

Reaction via a monomeric intermediate, where $C$ refers to the concentration of [2Fe–2S](GS)$_4$ cluster, and $N$ is Nfu protein monomer:

$$N + C \underset{k_{-1}}{\overset{k_1}{\rightleftharpoons}} NC$$
$$NC + N \xrightarrow{k_2} N_2C$$

By use of the steady state approximation, Eq. (1) is obtained.

$$\begin{aligned} & k_1[N][C] = k_{-1}[NC] + k_2[NC][N] \\ & [NC] = \frac{k_1[N][C]}{k_{-1}+k_2[N]} \\ \text{Rate} \quad & = k_2[NC][N] = \frac{k_1 k_2 [N]^2 [C]}{k_{-1}+k_2[N]} \\ \sim \quad & k_1[N][C] \qquad \text{when} \quad k_2[N] \gg k_{-1} \end{aligned} \tag{1}$$

Reaction via a dimeric intermediate:

$$2N \underset{k_{-1}}{\overset{k_1}{\rightleftharpoons}} N_2$$
$$N_2 + C \xrightarrow{k_2} N_2C$$

By use of the steady state approximation, Eq. (2) is obtained.

$$\begin{aligned} & k_1[N]^2 = k_{-1}[N_2] + k_2[N_2][C] \\ & [N_2] = \frac{k_1[N]^2}{k_{-1}+k_2[C]} \\ \text{Rate} \quad & = k_2[N_2][C] = \frac{k_1 k_2 [N]^2 [C]}{k_{-1}+k_2[C]} \\ \sim \quad & k_1[N]^2 \qquad \text{when} \quad k_2[C] \gg k_{-1} \end{aligned} \tag{2}$$

## Kinetics of Fe–S cluster extraction from holo Nfu by glutathione

Glutathione has been previously shown to extract the iron– sulfur cluster from holo ISU to form the [2Fe–2S](GS)$_4$ complex by monitoring the change in the charge transfer bands at 330 nm and 420 nm by UV–Vis spectrophotometry. Formation of [2Fe–2S](GS)$_4$ complex was demonstrated by ESI mass spectrometry on a Bruker Micro-TOF (ESI) spectrometer and data was analyzed by use of Data-Analysis software (Bruker) [20]. Holo Nfu demonstrated a larger change in absorbance at 420 nm than at 330 nm, and so transfer of the cluster from Nfu to glutathione was monitored at that wavelength. Argon-purged, reconstituted holo Nfu at 10 μM in 50 mM HEPES, 100 mM NaCl, pH 7.5 was incubated with an excess of GSH from 4 to 100-fold in an anaerobic cuvette and the absorbance at 420 nm on a Cary Win UV spectrophotometer was monitored every 2 min over the course of 1 h. The change in absorbance at 420 nm was plotted against time and fit to an exponential decay to obtain the $k_{obs}$. A control reaction for holo Nfu in the absence of excess GSH was carried out under the same conditions to account for inherent cluster instability.

## Kinetic cluster transfer experiments

Kinetic cluster transfer experiments were designed based on the cluster transfer experiments by Johnson and coworkers [30, 31]. Reactions were performed on a JASCO J-815 CD spectrophotometer in a 1 cm anaerobic quartz cuvette from 600 to 300 nm at a scan rate of 200 nm/min at 25 °C, with a 2 min interval between each accumulation. Reactions that reached completion within the first 10 min were analyzed over a 10 nm wavelength scale based on the peak of interest with 10 s intervals between accumulations. Spectra were

normalized based on the concentration of the [2Fe–2S] cluster, and were processed using JASCO Spectramanager II Analysis software and represented in Origin 7.0.

Reactions in 50 mM HEPES, 100 mM NaCl, pH 7.5 were prepared by degassing a mixture of 40 μM apo protein in 5 mM DTT, and transferred to an anaerobic cuvette via a gas tight syringe. Degassed holo protein at 40 μM was added to the cuvette to initiate the reaction. The concentration of [2Fe–2S] in the reaction for each holo protein prior to the reaction was determined via the calibration curve for iron quantification by the bathophenanthroline method [28, 29].

Kinetics of cluster transfer was analyzed by converting the change in CD signal to the percentage of cluster transferred. The percent of cluster transfer was estimated based on the CD signal obtained for the final target protein at the end of the reaction and comparing it to the CD spectrum for the holo form of the same protein after reconstitution for that concentration of cluster. The plot of time versus percent cluster transfer was fit to a first-order exponential function to obtain $k_{obs}$, which was then used to obtain the second-order rate constant.

## Results

### In vitro assembly of an iron–sulfur cluster bound Nfu

Previous reports on human Nfu have suggested binding of a [4Fe–4S] cluster [17] as well as redox activity for the conserved thioredoxin cysteine pair [18, 19], but no clear consensus has emerged concerning the in vivo function of the protein. Delivery of sulfide via enzymatic methods appears essential for successful Fe–S reconstitutions, since attempts with standard iron and sulfide salts failed [16, 18, 19]. However, human Nfu is readily reconstituted by use of *Tm* NifS and L-cysteine to generate a holo protein with a bound iron–sulfur cluster, the spectrum of which could be observed by both UV–Vis and CD spectroscopy (Fig. 1). Both of these techniques suggest the presence of a bound [2Fe–2S] cluster and are consistent with analytical quantitation data that support one $[2Fe–2S]^{2+}$ cluster per protein monomer by protein and iron quantification, with an overall reconstitution yield of ~75 % that is consistent with prior reports, if not far exceeding, for Nfu-type proteins [11, 13]. Both of these techniques suggest the presence of a bound [2Fe–2S] cluster.

The $\varepsilon_{420}$ value for Nfu dimer-bound [2Fe–2S] cluster is estimated to be 9.07 $mM^{-1}$ $cm^{-1}$, after accounting for reconstitution yield, which lies in the expected range of 7000–11,000 $M^{-1}$ $cm^{-1}$ based on published data [13, 32] and also matches the observed trend in absorbance. The characteristic UV peaks at 330 nm and 420 nm match the peaks observed for the homologous [2Fe–2S] cluster bound *Synechocystis* NifU [14] and *Arabidopsis thaliana* Nfu2 [13, 33, 34]. Similarly, the CD also spectrum resembles that of a [2Fe–2S]-bound protein, and is very similar to that of [2Fe–2S] cluster bound *Synechocystis* NifU (Figure S2) rather than a [4Fe–4S] cluster derivatives. Typically the latter are CD silent and require very high concentrations (>200 μM) to observe the weak spectral features, generally including a negative feature around 400 nm, as observed for NsrR [35], WhiD [36], *A. thaliana* Nfu2 with [4Fe–4S] bound [13], $SufB_2C_2$ and $SufBC_2D$ [37].

## Oligomeric state of holo Nfu

To determine the oligomeric state of holo Nfu, analytical ultracentrifugation (AUC) was performed. Initially, the apo protein at 50 μM was examined and found to exist in two states: a monomeric state at roughly 22 kDa, (expected molecular weight is 23.8 kDa) accounting for 45 % of the sample, and a dimeric state comprising 52 % (Fig. 2a). The remaining 3 % reflects higher-order aggregates. Since a dimer was present in such a high proportion, we also examined the protein's oligomeric state in the presence of 1 mM TCEP following 30 min of incubation. With TCEP, both the monomeric and dimeric states were still observed, but in slightly different ratios: 44 % monomer and 44 % dimer, indicating that the protein has a natural tendency to aggregate, but not as a result of disulfide bonding through the CXXC active site, consistent with other Nfu-type proteins [13, 34]. For the holo protein, the signal at 420 nm was monitored, which would only account for the holo protein contribution. In that case, dimeric and tetrameric forms were observed at 46.7 % and 51.6 %, respectively (Fig. 2b). Some higher-order oligomers were also observed for the homologous holo *Arabidopsis thaliana* Nfu2 protein [13], consistent with our results for human Nfu. Separation and isolation of the two holo species with analytical gel filtration resulted in UV and CD spectra similar to the spectral features shown in Fig. 1, further supporting the protein's natural tendency to oligomerize. Furthermore, the AUC experiments support our reconstitution yield as shown by the 280 nm trace for holo Nfu (Figure S3).

## Reconstitution of Nfu by the [2Fe–2S](GS)$_4$ complex

In addition to chemical reconstitution of human Nfu, the ability of human Nfu to take up an iron–sulfur cluster from a general pool of glutathione-bound iron–sulfur cluster [20] was examined by CD spectroscopy. Because the visible region CD spectra of biological Fe/S clusters are sensitive to the asymmetry of the cluster environment, CD spectroscopy is the method of choice for monitoring the kinetics of inter-protein iron–sulfur cluster transfer reactions [31, 38, 39]. Addition of the [2Fe–2S](GS)$_4$ complex, resulted in the appearance of the CD spectral signature for holo human Nfu (Fig. 1) over time (Fig. 3a). Following cluster uptake, the CD spectrum after cluster uptake was readily overlaid with that of the reconstituted holo human Nfu (Fig. 3a), indicating that in both cases, human Nfu has a similar cluster ligand environment and has the same form of bound cluster. The uptake of the cluster by Nfu was almost complete within the first 10 min (Fig. 3a). No further change in spectrum was observed after monitoring the reaction for an additional hour, suggesting that only one form of a bound iron–sulfur cluster was accessible under these conditions. Since the reaction was complete in such a short time frame, the reaction was monitored over a shorter time scale to better define the initial rate (Fig. 3a inset). No reaction was observed by mixing the apo protein with the same concentration of free iron, sulfide and glutathione, indicating that the chemically made intact cluster is the only method of reconstitution.

The kinetics of cluster uptake were monitored while varying both, cluster concentration and protein concentration, to determine the rate constants for the different kinetic reactions (Fig. 3b, 4). Variation of cluster concentration resulted in a reaction order of one for protein:cluster and a fitted second-order rate constant of 4900 ± 800 $M^{-1}$ $min^{-1}$ (Fig. 3b). The plot of $k_{obs}$ for cluster uptake versus total apo protein concentration resulted in an inverse rectangular hyberbola (Fig. 4). This can be fit to a substrate inhibition model, in

which the addition of more apo Nfu promotes the formation of Nfu dimers, causing the monomer concentration to decrease. However, the monomeric form is the active species capable of taking up the cluster. This trend is reflected by the observed hyperbolic decay in the uptake rate with increasing protein concentration, while dimerization is also consistent with the oligomeric states demonstrated in AUC (Fig. 2) and native PAGE gel experiments (Figure S4), which both confirm that the dimerization is not due to a disulfide bridge. As shown in Eq. (3), M corresponds to monomeric protein and $M_2$ is the dimeric form, which exists in equilibrium. The reaction mechanism is summarized by Eq. (4), which then yields Eq. (5) [40, 41],

$$M_2 \overset{K_D}{\rightleftharpoons} 2M, \quad (3)$$

$$M + [2Fe-2S](GS)_4 \xrightarrow[-2\,GSH]{k_1} M - [2Fe-2S](GS)_2 \xrightarrow[-2\,GSH]{M} M_2 - [2Fe-2S] \quad (4)$$

$$k_{obs} = k_1[P]/K_D + [P]\left(1 + \frac{[P]}{K_D}\right), \quad (5)$$

where $k_1$ is a first-order rate constant ($min^{-1}$), $P$ is the total protein concentration of Nfu, and $K_D$ is an apparent dissociation constant for the monomer–dimer equilibrium given by Eq. (6);

$$K_D = \frac{[M]^2}{[M_2]}. \quad (6)$$

The constants $k_1$ and $K_D$ were calculated directly from Eq. (5) by use of a non-linear least squares fit in Origin software. At lower protein concentration the plot of $k_{obs}$ versus protein concentration is linear and was used to obtain the second order rate constant for the formation of the holo protein, ~2500 ± 1200 $M^{-1}$ $min^{-1}$, which is comparable to the rate constant obtained by varying the cluster concentration. The first-order rate constant ($k_1$) was determined to be 1.0 $min^{-1}$ and the apparent dissociation constant ($K_D$) was 30 μM. The dependence of the rate of [2Fe–2S](GS)$_4$ cluster uptake was also determined in the presence of excess glutathione, as some iron–sulfur proteins, such as glutaredoxins utilize GSH as ligands for iron–sulfur cluster binding [38, 42]. However, excess GSH had no effect on the rate of [2Fe–2S](GS)$_4$ cluster uptake by human Nfu, even with a ten-fold excess.

The second-order rate constant for [2Fe–2S](GS)$_4$ cluster uptake by human Nfu was also determined by use of an alternative method, similar to that of Johnson and coworkers [13, 30, 31, 38]. Nfu and the [2Fe–2S](GS)$_4$ cluster were mixed in a 1:1 ratio at 50 μM each and

the percentage of cluster transfer was calculated from the CD data (Fig. 3), which was then fit to an exponential equation to obtain a $k_{obs}$. The $k_{obs}$ was then divided by the concentration of iron–sulfur cluster to determine the second-order rate constant as 1930 ± 212 $M^{-1}$ $min^{-1}$, which is in reasonable agreement with the second-order rate constant of 4900 $M^{-1}$ $min^{-1}$ noted above from concentration dependence experiments.

## Extraction of the iron–sulfur cluster by glutathione

Cluster exchange with the [2Fe–2S](GS)$_4$ complex could also be completed in the reverse direction in that GSH can extract the [2Fe–2S] cluster from reconstituted Nfu to form the [2Fe–2S](GS)$_4$ complex. Following incubation of 10 μM holo reconstituted human Nfu with 1 mM GSH, the peak at 420 nm for holo Nfu was observed to decrease, as monitored by UV–vis spectroscopy (Fig. 5). The decrease in peak intensity at 420 nm does not reflect simple degradation of cluster from the holo protein, as the control sample lacking GSH, demonstrated almost no change in absorbance at the same wavelength (Fig. 5). Cluster extraction is supported by the time-dependent change in the UV–Vis spectrum, where the concentration of cluster transferred can be calculated by use of the Beer-Lambert relationship because the extinction coefficients for the [2Fe–2S](GS)$_4$ complex [20] and holo human Nfu (this work) are known at 420 nm. From the absorbance change, the estimated [2Fe–2S](GS)$_4$ complex formed at the end of 1 h is 5.4 μM from an initial concentration of [2Fe–2S] cluster of 10 μM. This is consistent with the half-time determined for the reaction.

Further control reactions for [2Fe–2S](GS)$_4$ complex in 50 mM Hepes, 100 mM NaCl, pH 7.5 indicated no cluster breakdown at pH 7.5 over the course of 1 h (Figure S5), correlating well with the previous determination that the [2Fe–2S](GS)$_4$ complex is a physiologically relevant substrate in ABCB7 exporter proteoliposome assays [43]. The reaction mixture was then further analyzed using ESI mass spectrometry to demonstrate formation of [2Fe–2S](GS)$_4$ complex. An MS signature peak for the intact cluster was observed at 1427.3 (Figure S6). Other spectral peaks were observed at 1413.3 and 1435.3 corresponding to intermediate species previously identified in mass spectra of [2Fe–2S](GS)$_4$ complex [44], and also similar to reaction intermediates observed in the cluster assembly product for the scaffold proteins (IscS-IscU) [45]. The cluster intermediate is consistent with previous GSH extraction reactions performed in our lab [20, 44] and can be attributed to loss of a sulfur during the ionization process of ESI–MS.

Based on the absorbance change at 420 nm, in the presence of excess GSH, a second order rate constant of 130 ± 22 $M^{-1}$ $min^{-1}$ was determined for cluster transfer from holo Nfu to exogenous glutathione, to form [2Fe–2S](GS)$_4$ complex, which is significantly lower than the uptake rate constant of 1930 $M^{-1}$ $min^{-1}$.

## Cluster transfer from holo Nfu to apo ferredoxins

Exchange of protein-bound [2Fe–2S] cluster with free GSH is one potential function for Nfu, which would allow it to act as an iron–sulfur cluster storage protein when the concentration of GSH is low. However, we also investigated additional possible functional roles for human Nfu and observed rapid and complete cluster transfer from holo human Nfu

to apo human ferredoxins. The latter display well defined and highly conserved roles in iron–sulfur cluster biogenesis [24, 46, 47], with distinct CD signature peaks [39], and with precedence as model [2Fe–2S] target proteins [14, 28, 48]. The two human ferredoxins share 69 % similarity in protein sequence [24], but they serve very different physiological functions. Ferredoxin 1 plays an essential role in steroidogenesis, while ferredoxin 2 is involved in the biosynthesis of heme A and iron–sulfur cluster proteins [46].

The CD spectrum of holo ferredoxin 1 differs greatly from that of holo Nfu, again providing a favorable method to monitor cluster transfer when reconstituted holo human Nfu was added to an anaerobic mixture of apo human ferredoxin 1 (Fig. 6). By monitoring the change in CD signal with time, the percentage of cluster transfer from 40 μM Nfu-bound cluster to 40 μM apo ferredoxin 1 was readily calculated, based on the initial concentration of [2Fe–2S]. This provided a second-order rate constant for this reaction of 4695 ± 823 $M^{-1}$ $min^{-1}$. Similarly, cluster transfer from holo human Nfu to apo human ferredoxin 2 was monitored from the change in CD intensity (Fig. 6) and a second-order rate constant of 3849 ± 1242 $M^{-1}$ $min^{-1}$ was determined for [2Fe–2S] cluster transfer from Nfu to ferredoxin 2. The CD signal changed directly from the signal of holo Nfu to the holo ferredoxin signal, consistent with no additional reaction intermediate being formed in the process. No transfer was observed in the reverse direction, from either of the ferredoxins to Nfu. The rates obtained for the two observed unidirectional transfer reactions are within the realm of previously determined iron–sulfur cluster transfer rates [13, 30, 31, 48]. Additionally, they are also faster than the rates that have been determined for the transfer to apo *Azotobacter vinelandii* ferredoxin from either *A. vinelandii* IscU or Grx5. In those cases, the transfer rates were 800 $M^{-1}$ $min^{-1}$ for IscU in the presence of chaperones [48] and 2100 $M^{-1}$ $min^{-1}$ for Grx5 [31], suggesting that human Nfu can serve a general role as an iron–sulfur cluster transport protein based on its rapid iron–sulfur cluster transfer rates (Table S1).

## Discussion

Given the limited available knowledge of the cellular and functional roles of human Nfu, we have investigated the Fe–S cluster chemistry of the protein with regard to reconstitution and cluster transfer reactions. *In vitro* reconstitution mediated by *Tm* NifS, ferric chloride, and L-cysteine resulted in the formation of holo human Nfu, based on the characteristic iron–sulfur cluster charge transfer peaks observed in UV–Vis and CD spectra (Fig. 1). While human Nfu has previously been suggested to bind a [4Fe–4S] cluster [17], under the reconstitution conditions used in this report, we found holo Nfu to be a [2Fe–2S]-bound species as observed by signature [2Fe–2S] UV–Vis and CD spectra [13, 14, 17, 33–36, 39]. Both types of clusters have previously been found on Nfu-type proteins [11–14, 17, 34, 38]; however, we believe that reconstitution via enzymatic methods, such as those utilized in this work, more closely resemble the process of de novo cluster synthesis on IscU and therefore reflect more physiological reconstitution conditions [4]. Furthermore the ability of holo Nfu to efficiently take up and transfer a [2Fe–2S] cluster via the [2Fe–2S](GS)$_4$ complex (Fig. 3), and almost quantitatively transfer that cluster intact to ferredoxins without any indication of an intermediate species (Fig. 6), also supports the presence of a bound [2Fe–2S] cluster. We further investigated the nature of the cluster by performing an in-cuvette reconstitution of

apo Nfu and monitored the CD spectra over 4 h. No change in CD signature indicative of a [4Fe–4S] was observed.

We further sought to identify the oligomeric state in which Nfu can bind the [2Fe–2S] cluster. Apo Nfu was present in both monomeric and dimeric forms, indicating the inherent nature of the protein to dimerize (Fig. 2). Oligomerization was also observed for the holo protein, which is found to exist in both dimeric and tetrameric states (Fig. 2), consistent with other homologues of Nfu [13].

We have previously reported and characterized a glutathione-based [2Fe–2S] cluster that most likely exists in the cellular labile iron pool, and is readily formed by glutathione extraction of the [2Fe–2S] core from the ISU scaffold protein [20, 43]. This provides a biosynthetic pathway to formation of $[2Fe–2S](GS)_4$. This cluster can consequently be utilized to reconstitute other iron–sulfur cluster proteins, including the iron–sulfur cluster scaffold protein ISU [20]. We also describe herein how human Nfu can be reconstituted using this $[2Fe–2S](GS)_4$ complex with a second-order rate constant of 1930 $M^{-1}$ $min^{-1}$ (Fig. 3) that is similar to transfer reactions that have been observed between other iron–sulfur cluster proteins [13, 30].

Based on available data, uptake of cluster appears to be first-order in $[2Fe–2S](GS)_4$ complex and in protein (Eq. 1). This supports direct cluster uptake by monomeric protein, presumably at the dithiol site, with retention of two terminal glutathione ligands (Fig. 7). Subsequent displacement of these by another monomeric Nfu yields a dimeric protein with bridging [2Fe–2S] cluster. The propensity of the protein to aggregate, promotes dimer-tetramer equilibrium, with no appreciable concentration of the intermediate monomeric holo Nfu, with cluster stabilized by binding of two exogenous glutathione molecules (Fig. 7).

The alternative mechanism in which dimeric apo Nfu directly takes up $[2Fe–2S](GS)_4$ to form the [2Fe–2S] bridged dimer, illustrated in Fig. 8, can be excluded; this mechanism would require two Nfu proteins to form a prereaction complex (Eq. 2) and is not supported by the behavior observed for the protein dependence for holo Nfu formation (Fig. 4).

Recent studies have suggested formation of Fe–S cluster-associated high molecular weight species (HMWS) when excess DTT is added to the reaction mixtures after the formation of [2Fe–2S] clusters, which can then either facilitate cluster transfer between putative protein partners or formation of [4Fe–4S] cluster on scaffold proteins [49, 50]. To investigate the role of DTT in our studies, several control reactions were performed by incubating $[2Fe–2S](GS)_4$ complex, holo Nfu and holo ferredoxins with excess DTT. No change was observed in UV–vis or CD spectra for either $[2Fe–2S](GS)_4$ complex (Figure S5) or holo ferredoxins (Figures S7 and S8), clearly indicating that under our conditions, DTT does not form any intermediate Fe–S species. In the case of holo Nfu, a minimal change was observed in the CD signal (<10 %) when incubated with excess DTT (Figure S9). In addition, the change is inconsistent over time indicating non-specific interaction of DTT with the holo protein. Similarly, the transfer reactions were repeated in the presence of 5 mM TCEP instead of 5 mM DTT and comparable second-order rate constants were obtained (data not shown).

Similar to uptake of the [2Fe–2S](GS)$_4$ complex by apo Nfu, we investigated the ability of free GSH to extract the bound cluster from holo reconstituted Nfu to re-form the [2Fe–2S](GS)$_4$ complex (Fig. 5). The rate constant for GSH extraction of the cluster from Nfu is significantly lower than the rate constant obtained for cluster uptake by Nfu, suggesting that the equilibrium between iron–sulfur cluster bound Nfu and the pool of [2Fe–2S](GS)$_4$ complex favors holo Nfu. The actual cellular concentrations of the protein and the [2Fe–2S](GS)$_4$ complex, and the downstream protein targets for cluster transfer from Nfu, would dictate where the equilibrium lies in vivo.

We have also examined cluster exchange and/or delivery to and from apo protein targets. Holo human Nfu was shown to deliver its [2Fe–2S] cluster to both of the apo human ferredoxins (Fdx1 and Fdx2), which are unable to directly take up cluster from the [2Fe–2S](GS)$_4$ complex. The rate constant for transfer to ferredoxin 1 was slightly faster than for transfer to ferredoxin 2 (Fig. 6; Table 1), and both of these transfer reactions demonstrated larger rate constants relative to the transfers to *A. vinelandii* ferredoxin from either IscU or Grx5 (Table S1) [31, 48]. The relatively fast transfer rate from human Nfu supports a role for Nfu in delivery of iron–sulfur clusters to apo protein targets. Given this new role for human Nfu we are currently examining potential partner proteins for cluster transfer reactivity that will allow us to discern potential networks of cellular iron–sulfur cluster trafficking pathways, as well as expanding on the physiological role for Nfu as an iron–sulfur scaffold and delivery protein. Human Nfu has been recently implicated in delivery of a [4Fe–4S] cluster to the apo target protein lipoate synthase (LIAS) [8–10]. It remains unclear if this is promoted by direct transfer from Nfu to LIAS, or via intermediate cluster carriers. It is also unclear if the [4Fe–4S] clusters result from prior formation of a [4Fe–4S] center that is finally delivered to LIAS, or if by consecutive delivery of [2Fe–2S] centers with condensation to the [4Fe–4S] form. In the former case, it is also uncertain if the [4Fe–4S] center, on whatever protein is involved, is formed directly or by sequential delivery of two [2Fe–2S] centers. Alternatively under different reconstitution conditions, human Nfu may be able to bind both types of iron–sulfur clusters and mediate their delivery to various apo targets as needed based on cellular conditions. The data in hand supports a [2Fe–2S] form as the dominant cluster type for human Nfu.

In this report, we have demonstrated apo Nfu to accept a [2Fe–2S] cluster from a glutathione-complexed [2Fe–2S] core, most likely via a monomeric intermediate. A potential functional role for a [2Fe–2S] cluster bound human Nfu, has been demonstrated in as much as it can deliver its iron–sulfur cluster to apo target ferredoxins, suggesting that Nfu may also function downstream of Grx5 in the mitochondria to deliver clusters to target proteins [4]. The ability to transfer this [2Fe–2S] cluster to apo [4Fe–4S] target proteins, similar to the ability of ISU to assemble [4Fe–4S] clusters on targets such as aconitase [51], is also a possibility that we are currently exploring. Nevertheless, we have demonstrated that human Nfu can bind a [2Fe–2S] cluster, and that this [2Fe–2S] cluster can be exchanged with GSH and the physiologically relevant [2Fe–2S](GS)$_4$ complex, with subsequent delivery to target apo human ferredoxins. This establishes Nfu as a likely central mediator of cluster transfer chemistry in both the mitochondrion and cytosol.

## Supplementary Material

Refer to Web version on PubMed Central for supplementary material.

## Acknowledgments

We thank Dr. Marina Bakhtina for her assistance with analytical ultracentrifugation experiments. This work was supported by a grant from the National Institutes of Health [AI072443]. Christine Wachnowsky was supported by an NIH Chemistry/Biology Interface training grant (T32 GM095450).

## Abbreviations

| | |
|---|---|
| **AUC** | Analytical ultracentrifugation |
| **CD** | Circular dichroism |
| **ESI-MS** | Electrospray ionization mass spectrometry |
| **Fdx** | Ferredoxin |
| **GSH** | Glutathione |
| **MMDS1** | Multiple mitochondrial dysfunctional syndrome 1 |

## References

1. Lill R, Muehlenhoff U. Annu Rev Biochem. 2008; 77:669–700. [PubMed: 18366324]
2. Qi W, Cowan JA. Coord Chem Rev. 2011; 255:688–699. [PubMed: 21499539]
3. Johnson DC, Dean DR, Smith AD, Johnson MK. Annu Rev Biochem. 2005; 74:247–281. [PubMed: 15952888]
4. Stehling O, Wilbrecht C, Lill R. Biochimie. 2014; 100:61–77. [PubMed: 24462711]
5. Ye H, Rouault TA. Biochemistry. 2010; 49:4945–4956. [PubMed: 20481466]
6. Ganesh S. Hum Mol Gen. 2003; 12:2359–2368. [PubMed: 12915448]
7. Ahting U, Mayr JA, Vanlander AV, Hardy SA, Santra S, Makowski C, Alston CL, Zimmermann FA, Abela L, Plecko B, Rohrbach M, Spranger S, Seneca S, Rolinski B, Hagendorff A, Hempel M, Sperl W, Meitinger T, Smet J, Taylor RW, Van Coster R, Freisinger P, Prokisch H, Haack TB. Front Genet. 2015; 6:123. doi:10.3389/fgene.2015.00123. [PubMed: 25918518]
8. Cameron Jessie M, Janer A, Levandovskiy V, MacKay N, Rouault Tracey A, Tong W-H, Ogilvie I, Shoubridge Eric A, Robin-sonBrian H. Am J Hum Genet. 2011; 89:486–495. [PubMed: 21944046]
9. Ferrer-Cortès X, Font A, Bujan N, Navarro-Sastre A, Matalonga L, Arranz JA, Riudor E, del Toro M, Garcia-Cazorla A, Campistol J, Briones P, Ribes A, Tort F. J Inherit Met Dis. 2012; 36:841–847.
10. Navarro-Sastre A, Tort F, Stehling O, Uzarska Marta A, Arranz José A, del Toro M, Labayru MT, Landa J, Font A, Garcia-Villoria J, Merinero B, Ugarte M, Gutierrez-Solana Luis G, Campistol J, Garcia-Cazorla A, Vaquerizo J, Riudor E, Briones P, Elpeleg O, Ribes A, Lill R. Am J Hum Genet. 2011; 89:656–667. [PubMed: 22077971]
11. Py B, Gerez C, Angelini S, Planel R, Vinella D, Loiseau L, Talla E, Brochier-Armanet C, Garcia Serres R, Latour J-M, Ollagnierde Choudens S, Fontecave M, Barras F. Mol Microbiol. 2012; 86:155–171. [PubMed: 22966982]
12. Angelini S, Gerez C, Choudens SOD, Sanakis Y, Fontecave M, Barras F, Py B. J Biol Chem. 2008; 283:14084–14091. [PubMed: 18339628]
13. Gao H, Subramanian S, Couturier J, Naik SG, Kim S-K, Leustek T, Knaff DB, Wu H-C, Vignols F, Huynh BH, Rouhier N, Johnson MK. Biochemistry. 2013; 52:6633–6645. [PubMed: 24032747]
14. Nishio K, Nakai M. J Biol Chem. 2000; 275:22615–22618. [PubMed: 10837463]

15. Li J, Ding S, Cowan JA. Biochemistry. 2013; 52:4904–4913. [PubMed: 23796308]
16. Liu Y, Cowan JA. Biochemistry. 2009; 48:7512–7518. [PubMed: 19722697]
17. Tong WH, Jameson GNL, Huynh BH, Rouault TA. Proc Natl Acad Sci USA. 2003; 100:9762–9767. [PubMed: 12886008]
18. Liu Y, Qi W, Cowan JA. Biochemistry. 2009; 48:973–980. [PubMed: 19146390]
19. Liu Y, Cowan JA. Chem Commun. 2007:3192–3194.
20. Qi W, Li J, Chain CY, Pasquevich GA, Pasquevich AF, Cowan JA. J Am Chem Soc. 2012; 134:10745–10748. [PubMed: 22687047]
21. Nuth M, Yoon T, Cowan JA. J Am Chem Soc. 2002; 124:8774–8775. [PubMed: 12137512]
22. Mansy SS, Xiong Y, Hemann C, Hille R, Sundaralingam M, Cowan JA. Biochemistry. 2002; 41:1195–1201. [PubMed: 11802718]
23. Xia B, Cheng H, Bandarian V, Reed GH, Markley JL. Biochemistry. 1996; 35:9488–9495. [PubMed: 8755728]
24. Qi W, Li J, Cowan JA. Dalton Trans. 2013; 42:3088–3091. [PubMed: 23208207]
25. Krebs C, Agar JN, Smith AD, Frazzon J, Dean DR, Huynh BH, Johnson MK. Biochemistry. 2001; 40:14069–14080. [PubMed: 11705400]
26. Lamm O. Ark Mat Astr Fys. 1929; 21B:1–4.
27. Schuck P. Biophys J. 2000; 78:1606–1619. [PubMed: 10692345]
28. Wu S-P, Wu G, Surerus KK, Cowan JA. Biochemistry. 2002; 41:8876–8885. [PubMed: 12102630]
29. Moulis J-M, Meyer J. Biochemistry. 1982; 21:4762–4771. [PubMed: 6753926]
30. Mapolelo DT, Zhang B, Randeniya S, Albetel A-N, Li H, Couturier J, Outten CE, Rouhier N, Johnson MK. Dalton Trans. 2013; 42:3107. [PubMed: 23292141]
31. Shakamuri P, Zhang B, Johnson MK. J Am Chem Soc. 2012; 134:15213–15216. [PubMed: 22963613]
32. Bandyopadhyay S, Naik SG, O'Carroll IP, Huynh BH, Dean DR, Johnson MK, Dos Santos PC. J Biol Chem. 2008; 283:14092–14099. [PubMed: 18339629]
33. Leon S, Touraine B, Ribot C, Briat J-F, Lobreaux S. Biochem J. 2003; 371:823–830. [PubMed: 12553879]
34. Yabe T. Plant Cell. 2004; 16:993–1007. [PubMed: 15031412]
35. Crack JC, Munnoch J, Dodd EL, Knowles F, Al Bassam MM, Kamali S, Holland AA, Cramer SP, Hamilton CJ, Johnson MK, Thomson AJ, Hutchings MI, Le Brun NE. J Biol Chem. 2015; 290:12689–12704. [PubMed: 25771538]
36. Crack JC, den Hengst CD, Jakimowicz P, Subramanian S, Johnson MK, Buttner MJ, Thomson AJ, Le Brun NE. Biochemistry. 2009; 48:12252–12264. [PubMed: 19954209]
37. Chahal HK, Outten FW. J Inorg Biochem. 2012; 116:126–134. [PubMed: 23018275]
38. Bandyopadhyay S, Gama F, Molina-Navarro MM, Gualberto JM, Claxton R, Naik SG, Huynh BH, Herrero E, Jacquot JP, Johnson MK, Rouhier N. EMBO J. 2008; 27:1122–1133. [PubMed: 18354500]
39. Stephens PJ, Thomson AJ, Dunn JBR, Keiderling TA, Rawlings J, Rao KK, Hall DO. Biochemistry. 1978; 22:4770–4778.
40. Segel, IH. Enzyme kinetics: behavior and analysis of rapid equilibrium and steady state enzyme systems. Wiley; New York: 1975.
41. Bisswanger, H. Enzyme kinetics: principles and methods. Wiley-VCH; Weinheim: 2002.
42. Picciocchi A, Saguez C, Boussac A, Cassier-Chauvat C, Chauvat F. Biochemistry. 2007; 46:15018–15026. [PubMed: 18044966]
43. Li J, Cowan JA. Chem Commun. 2015; 51:2253–2255.
44. Qi W, Li J, Chain CY, Pasquevich GA, Pasquevich AF, Cowan JA. Chem Commun. 2013; 49:6313.
45. Marinoni EN, de Oliveira JS, Nicolet Y, Raulfs EC, Amara P, Dean DR, Fontecilla-Camps JC. Angew Chem Int Ed Engl. 2012; 51:5439–5442. [PubMed: 22511353]
46. Sheftel AD, Stehling O, Pierik AJ, Elsässer H-P, Mühlenhoff U, Webert H, Hobler A, Hannemann F, Bernhardt R, Lill R. Proc Natl Acad Sci USA. 2010; 107:11775–11780. [PubMed: 20547883]

47. Webert H, Freibert S-A, Gallo A, Heidenreich T, Linne U, Amlacher S, Hurt E, Mühlenhoff U, Banci L, Lill R. Nat Commun. 2014; 5:5013. [PubMed: 25358379]
48. Chandramouli K, Johnson MK. Biochemistry. 2006; 45:11087–11095. [PubMed: 16964969]
49. Fox NG, Chakrabarti M, McCormick SP, Lindahl PA, Barondeau DP. Biochemistry. 2015; 54:3871–3879. [PubMed: 26016389]
50. Vranish JN, Russell WK, Yu LE, Cox RM, Russell DH, Baron-deau DP. J Am Chem Soc. 2015; 137:390–398. [PubMed: 25478817]
51. Unciuleac M-C, Chandramouli K, Naik S, Mayer S, Huynh BH, Johnson MK, Dean DR. Biochemistry. 2007; 46:6812–6821. [PubMed: 17506526]

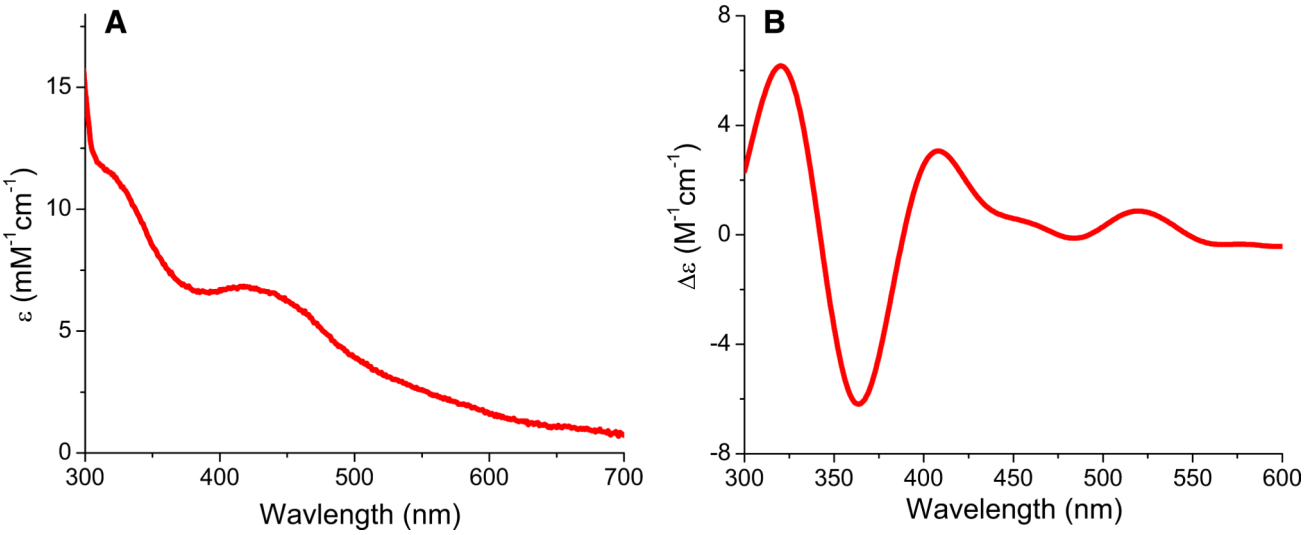


**Fig. 1.**

UV (**a**) and CD (**b**) spectra of [2Fe–2S] cluster-bound Nfu following in vitro reconstitution. All $\varepsilon$ and $\Delta\varepsilon$ values were calculated based on the monomeric protein concentration

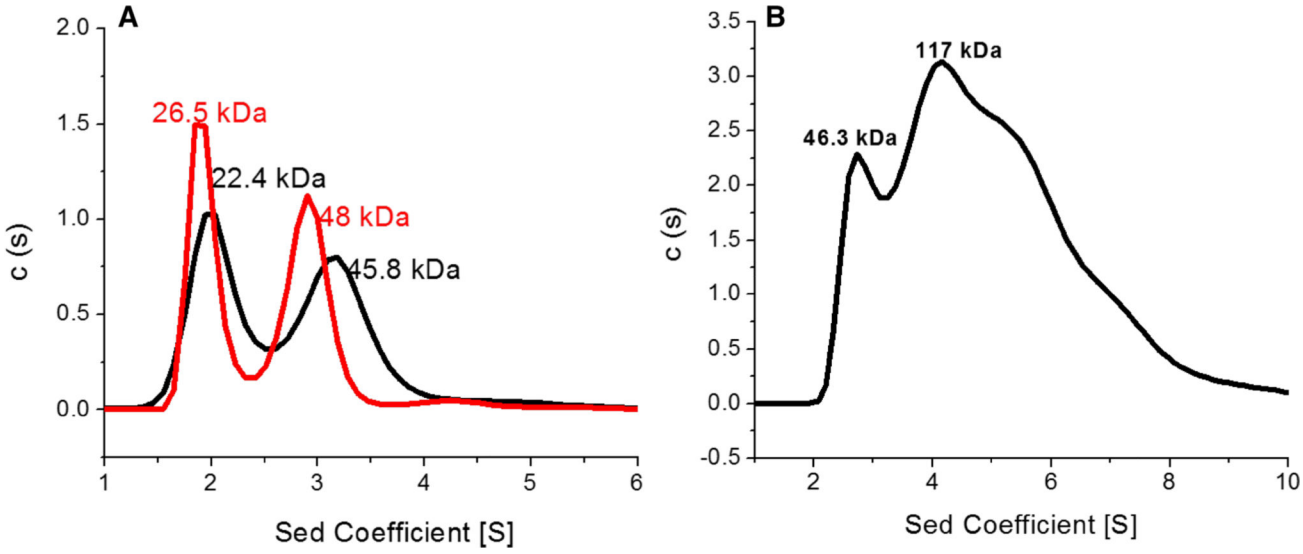


**Fig. 2.**

Analytical ultracentrifugation profiles of 50 μM Nfu. **a** Apo Nfu was sedimented in the absence (in *black*) and the presence (*red*) of 1 mM TCEP and monitored at 280 nm. Sedimentation profiles were fit to the Lamm equation [26, 27] using a continuous distribution model to obtain the molecular weights shown above the peaks. **b** Holo Nfu was monitored for sedimentation at 420 nm. The sedimentation data were fit in the same way as the apo protein

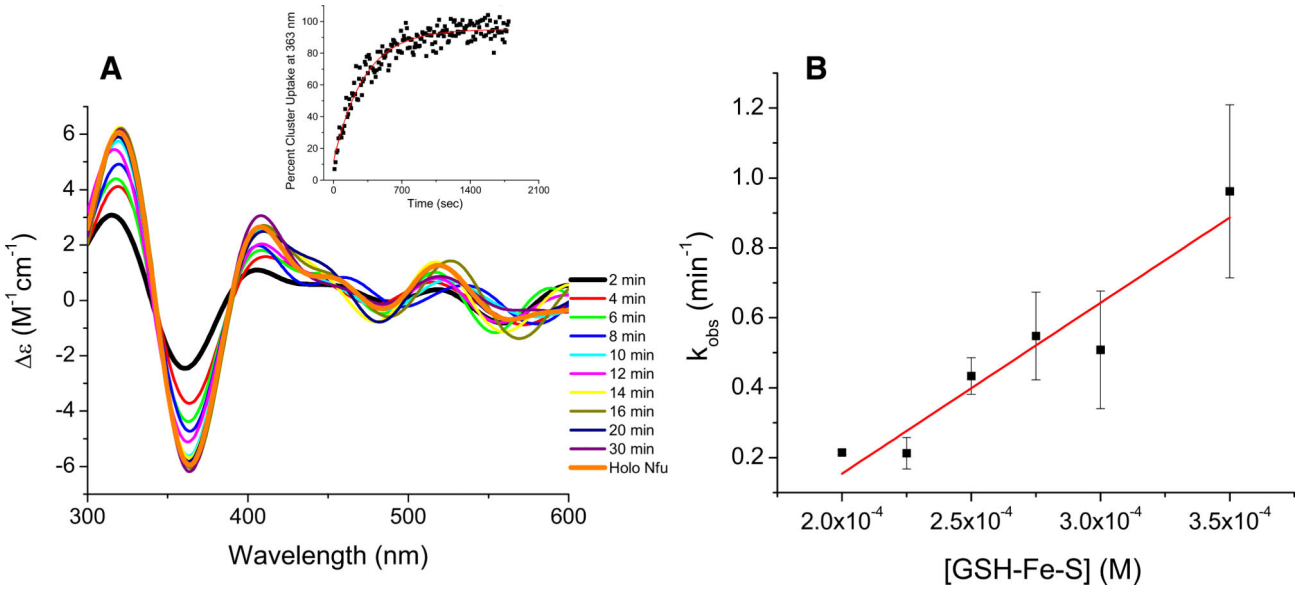


**Fig. 3.**

Determination of second-order rate constants for cluster transfer reactions from [2Fe–2S](GS)$_4$ complex to apo Nfu by use of CD spectroscopy. The decrease in $\Delta\varepsilon$ at 363 nm was monitored every 10 s to generate the *inset* (**a**), which was fit with an exponential to yield $k_{obs}$. From $k_{obs}$, the second-order rate constant was determined based on the [2Fe–2S](GS)$_4$ cluster concentration, yielding a rate constant of 1930 ± 212 $M^{-1}$ $min^{-1}$ for cluster uptake. **b** The initial rate of cluster uptake by 50 μM Nfu at different [2Fe–2S](GS)$_4$ complex concentrations was plotted against cluster concentration, which was varied from 200 to 400 μM, and fit linearly to obtain the second order rate constant which was determined to be 4900 ± 800 $M^{-1}$ $min^{-1}$

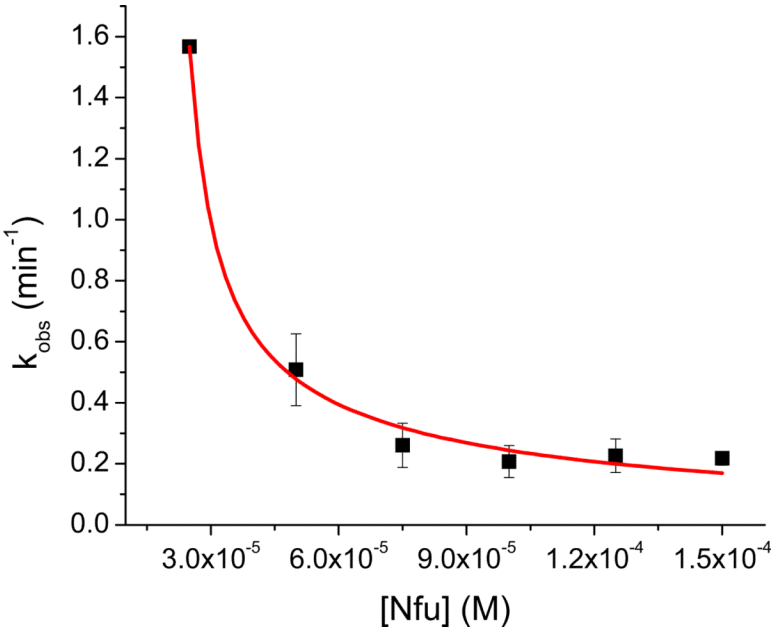


**Fig. 4.**

Dependence of the rate of cluster uptake by Nfu on protein concentration. The [2Fe–2S](GS)$_4$ cluster was kept in excess and held constant to maintain pseudo-first order conditions. The concentration of Nfu was varied from 25 to 150 μM, while the cluster concentration was kept constant at 300 μM, and the data was fit to Eq. (5), reflecting inhibition by the dimeric form of the protein. The second-order rate constant determined from the protein dependence for cluster uptake was 2500 ± 1200 $M^{-1}$ $min^{-1}$

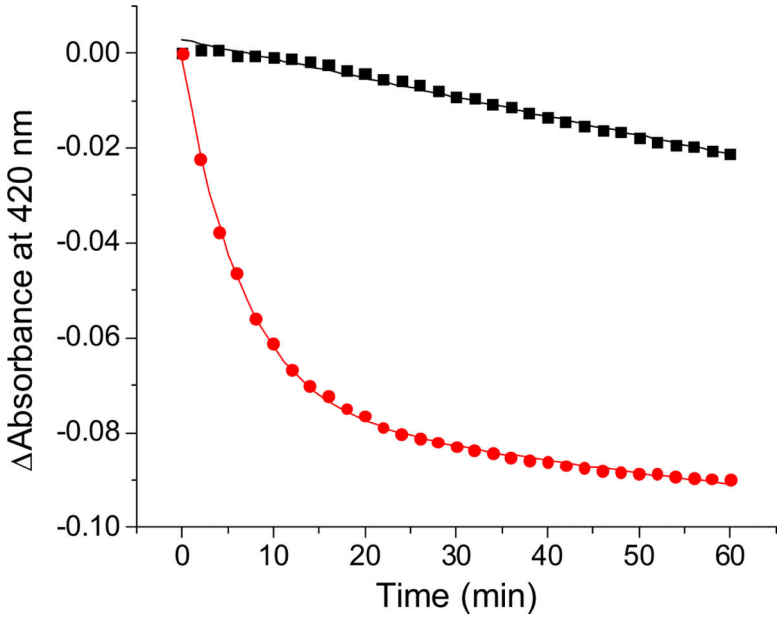


**Fig. 5.**

Extraction of the [2Fe–2S] cluster from reconstituted holo human Nfu (10 μM in cluster) to form the [2Fe–2S](GS)$_4$ complex monitored by UV–Vis at 420 nm. Stability of the holo protein was examined in the absence of glutathione as a control (*black*), while the experimental time-dependence for cluster extraction with a 100-fold excess of GSH is shown in *red*. For the latter fit, the equation includes both exponential and linear terms, where the linear term accommodates general background cluster degradation, resulting in a second-order rate constant of 130 ± 22 $M^{-1}$ $min^{-1}$, with no dependence on glutathione concentration

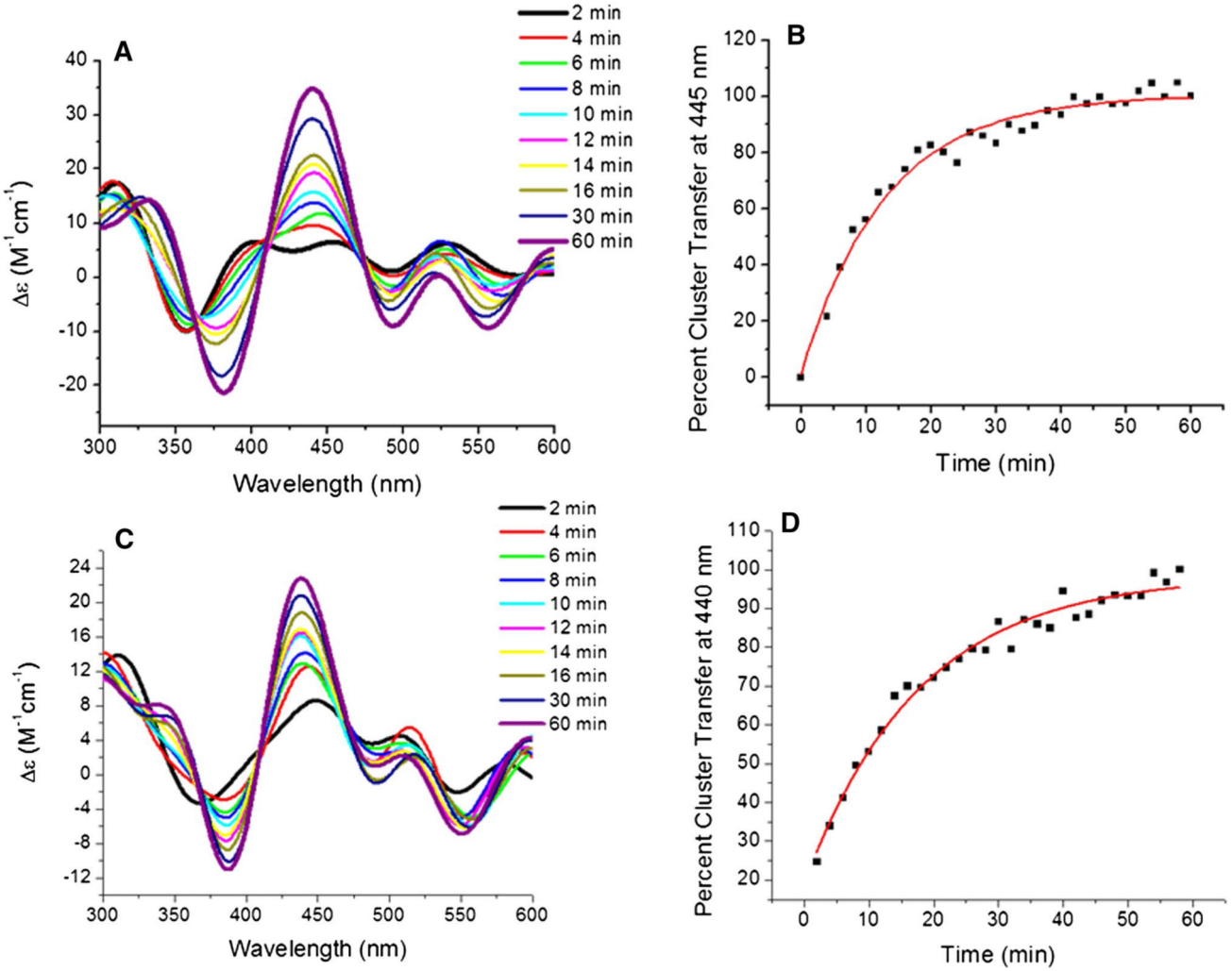


**Fig. 6.**

Kinetics of cluster transfer from holo Nfu to apo ferredoxins. **a** Time course of cluster transfer from holo human Nfu to apo human ferredoxin 1 recorded by CD in 50 mM HEPES, 100 mM NaCl, pH 7.5 at a 1:1 concentration ratio. Spectra were recorded every 2 min after the addition of holo Nfu, and converted to percent cluster transfer **b** to calculate the second order rate constant of 4695 ± 823 $M^{-1}$ $min^{-1}$ based on the concentration of the [2Fe–2S] cluster. **c** Time course of cluster transfer from holo human Nfu to apo human ferredoxin 2 recorded by CD under the same conditions as for ferredoxin 1. **d** The CD signal was again converted to the percentage of cluster transferred with time to calculate a second order rate constant of 3849 ± 1242 $M^{-1}$ $min^{-1}$

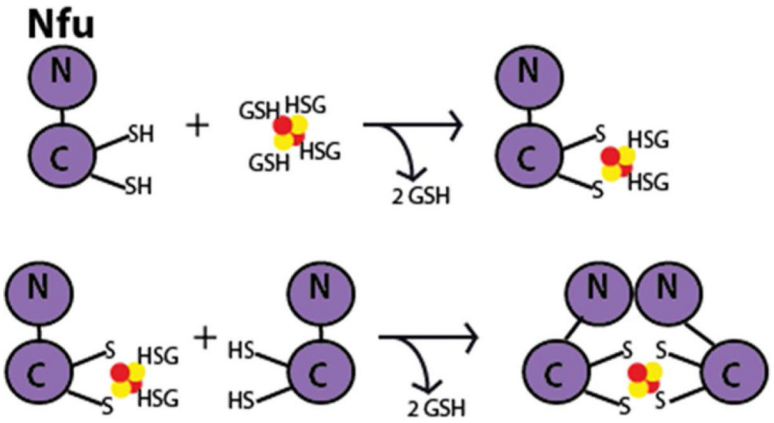


**Fig. 7.**

Model for [2Fe–2S] cluster uptake by monomeric Nfu, represented by the N- and C-terminal domains, from the $[2Fe–2S](GS)_4$ cluster complex to form an intermediate [2Fe–2S] species with two exogenous GSH ligands. A second monomeric Nfu displaces the GSH molecules to form [2Fe–2S] dimeric Nfu

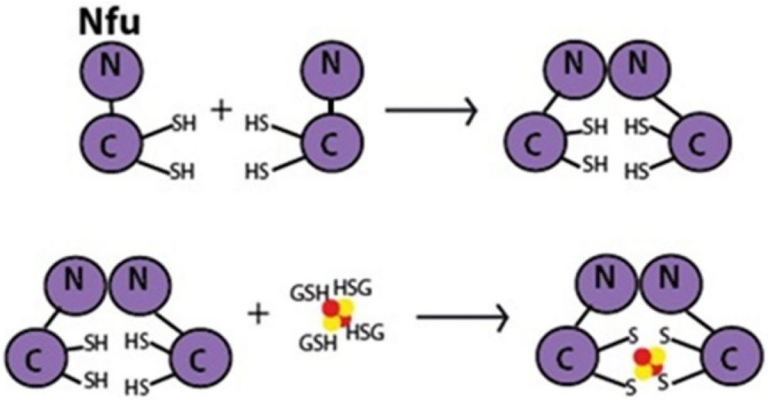


**Fig. 8.**

Model for direct [2Fe–2S] cluster uptake by pre-formed dimeric Nfu, shown by the N- and C-terminal domains, from the $[2Fe–2S](GS)_4$ cluster complex

**Table 1**

Summary of Nfu transfer rates determined in this work

| Transfer reaction | Rate ($M^{-1}$ $min^{-1}$) |
|---|---|
| [2Fe–2S](GS)$_4$ to apo human Nfu | 1930 ± 212 |
| Holo Nfu to [2Fe–2S](GS)$_4$ via GSH extraction | 130 ± 22 |
| Holo Nfu to apo Fdx1 | 4695 ± 823 |
| Holo Nfu to apo Fdx2 | 3849 ± 1242 |